Leaf Temperature Measurement Using Low-Resolution Thermal Camera Based on Thresholding and Clustering Techniques

Aryuanto Soetedjo[1*] and Evy Hendriarianti[2]
[1]Department of Electrical Engineering, Faculty of Industrial Engineering,
National Institute of Technology (ITN)
Malang, Indonesia 65145
[1]Department of Environmental Engineering, Faculty of Civil Engineering and Planning,
National Institute of Technology (ITN)
Malang, Indonesia 65145
Email: [1]aryuanto@lecturer.itn.ac.id, [2]evyhendriarianti@lecturer.itn.ac.id

***Abstract*—Leaf temperature can indicate photosynthetic rates, leaf water status, and stomata conductance. Leaf temperature can be measured using thermal resistance sensors, thermocouple devices, infrared thermometers, or infrared thermal imaging devices. Additionally, measuring leaf temperature using a thermal camera is simple and efficient. Therefore, the research proposes a leaf temperature measurement method using AMG8833, a low-resolution (64 pixels) thermal camera. The proposed system adopts an image segmentation technique to extract the leaf area from a thermal image. The leaf temperature is then calculated by averaging the temperature values on the leaf area. The proposed system aims to utilize a low-cost and low-resolution thermal camera for measuring the leaf temperature. The proposed approach is evaluated using real images of the Dieffenbachia plant, a popular ornamental plant that can be easily planted. In the experiments, fourteen segmentation methods consisting of eight thresholding techniques and six clustering techniques are evaluated. The experimental findings on the Dieffenbachia plant indicate that the most accurate leaf temperature measurements are obtained using local thresholding with an absolute error of 0.0109 and k-means clustering with an absolute error of 0.0134. The proposed method provides a simple, effective, and low-cost leaf temperature measurement system compared to the existing systems which employ high-cost commercial thermal cameras and complex measurement methods.**

***Index Terms*—Leaf Temperature Measurement, Low-Resolution Thermal Camera, Thresholding Techniques, Clustering Techniques**

Received: Oct. 20, 2023; received in revised form: Feb. 28, 2024; accepted: Feb. 28, 2024; available online: April 29, 2024.
*Corresponding Author

I. Introduction

LEAF temperature provides information on plant metabolism [1, 2] and water-use efficiency [3, 4]. Hence, it affects the photosynthetic response of plants [5]. Moreover, leaf temperature varies depending on plant physiology, ambient air temperature, wind, and solar irradiation. Leaf temperature can be measured using thermal resistance sensors, thermocouple devices, infrared thermometers, or infrared thermal imaging devices.

Thermal resistance is a high-precision and simple leaf temperature measurement device. However, the resistance is highly affected by environmental noise. Meanwhile, a thermocouple is a simple, high-precision leaf temperature measurement device. However, it has a long response time. It is also affected by the leaf environment. Furthermore, because both devices must be installed at the leaf surface, they are infeasible for measuring numerous leaves [6].

Next, an infrared thermometer measures leaf temperature without contact by detecting the infrared radiation emitted by the leaves, which is then converted into temperature readings. This device is known for its high accuracy and sensitivity, but its performance can be influenced by the distance from the target and the surrounding environmental temperature [6]. Similar to infrared thermometers, infrared thermal imaging uses infrared radiation. However, the emitted infrared radiation is converted into a thermal image rather than being converted into temperature. It displays the temperature distribution in the spatial area of the object under observation. The main drawbacks of infrared thermal imaging are its high cost and low precision [6].

TABLE I
LEAF SEGMENTATION PERFORMANCE OF VISIBLE, INFRARED, AND THERMAL IMAGES [7].

Images	Recall	Precision	F1 Score
Visible	0.934	0.751	0.794
Infrared	0.868	0.575	0.599
Thermal	0.926	0.494	0.394

Previous research compares leaf segmentation techniques to visible, infrared, and thermal images [7]. The thermal images perform the worst, as listed in Table I. However, since the leaf temperature measurement considers the average values of the pixels in a segmented image [6], it suggests that thermal images can be used effectively.

Leaf temperature measurements using a thermal camera can be divided into three categories according to the measurement area: a) spot measurement, b) a few leaves of the plant, and c) large leaf area. The research deals with the second category, in which the leaf temperature is calculated using a thermal camera whose pixels belong to the detected leaf. In previous research, a thermal camera is used to measure the canopy temperatures of horticultural plants for irrigation scheduling [8]. Moreover, thermal imaging systems are used to detect plant diseases [9]. A precise leaf thermal-sensing method has also been developed for smart greenhouse farming [10].

Leaf-temperature measurements using thermal cameras typically employ hand-type, platform-mounted, or embedded cameras. Hand-type thermal cameras are medium- and high-cost cameras and display devices attached to handheld instruments [11, 12]. Meanwhile, platform-mounted thermal cameras offer medium resolution at a high cost [13, 14]. These cameras are affixed to a platform or vehicle, while the display device is positioned separately. Then, embedded thermal cameras have a low resolution and are inexpensive. The camera module should be interfaced with an embedded system for access and visualization [15–17].

Several studies have explored thermal cameras. For example, FLIR Vue Pro R is used to measure the grapevine leaf temperature. The Red Green Blue (RGB) camera simultaneously captures the leaves. Then, image-processing techniques are employed to extract the leaf area from the RGB image. Then, the average temperature in the corresponding leaf area in the thermal image is computed to calculate The Crop Water Stress Index (CWSI) [14]. Next, an embedded thermal camera FLIR Lepton 3.5 and an RGB Raspberry Pi camera are connected to a Raspberry Pi 4 Model B to measure crop canopy temperature. Leaf area is detected from the RGB image using a segmentation technique. The corresponding pixels in the thermal image are used to calculate leaf temperature [15]. A similar system has also been developed, in which RGB thermal images and minimum and maximum leaf temperatures are sent to the web [16]. Moreover, a low-cost thermal sensor, MLX90620, is connected to an Arduino MEGA 2560 to measure the olive tree canopy temperature. The device measured the canopy temperature at a distance of 1 m over a measurement area of 75 cm $\times$ 10 cm [17].

Clustering is a method of grouping objects according to their similarity within a group. Agglomerative clustering starts with the points as individual clusters [18]. Subsequently, in each iteration, it merges two closed clusters based on cluster proximity. In the Agglomerative Ward method, cluster proximity is defined based on the squared error that occurs when two clusters are merged. In average agglomeration, cluster proximity is defined as the average distance of pairwise points in different clusters.

Balanced iterative reduction and clustering using hierarchies (Birch) is a clustering technique based on Clustering Features (CF) and CF trees [18]. The algorithm comprises four main phases. The first phase involves loading data into memory by building a CF tree. In the second phase, a smaller CF tree is built. Global Agglomerative clustering is performed in the third phase. The fourth phase refines the clusters obtained in the previous phase.

The mixture model assumes that the clusters have different Gaussian distributions [18]. The parameters of the mixture models are estimated using the Expectation-Maximization (EM) algorithm. The probability of each object belonging to each distribution is calculated during the expectation step. The parameters are updated to maximize the expected likelihood in the maximization step.

K-means clustering is a simple and widely used method. It begins with K points as the initial centroids [18]. In each iteration, each point is assigned a closed centroid. The centroid is updated according to the points belonging to the cluster.

Spectral clustering is a method that defines clusters based on a similarity graph. The algorithm begins by creating a similarity graph for the objects to cluster [18]. It then creates the k-first eigenvectors of the Laplacian graph to define a feature vector. Finally, the k-means algorithm is applied to find k-clusters from the features.

The main challenge is determining the leaf area detected from the image. Existing systems typically use a combination of RGB and thermal cameras [14, 15] or manual selection using image software tools [19]. In the proposed system, rather than using an RGB

camera or manual selection, the researchers propose using a thermal image directly for leaf area detection by applying leaf segmentation techniques based on thresholding and clustering. A low-cost thermal camera (AMG8833) is used. This camera is a suitable thermal image sensor module for interfacing embedded systems for real-time applications such as people counting [20], occupancy detection [21], and personal thermal comfort modeling [22]. Therefore, the proposed thermal camera system offers an affordable real-time leaf temperature monitoring system.

The main contributions of the research are as follows. First, the researchers propose a simple and effective method for calculating leaf temperature using a low-resolution thermal camera. Second, they compare several segmentation techniques, namely thresholding and k-means clustering methods, for segmenting leaf objects using a thermal camera. Last, the proposed system provides a low-cost device for real-time monitoring of leaves.

II. Research Method

A. Thermal Image Data Acquisition

Data collection is conducted over five days. Then, data from the measurement unit are sent to the cloud-Supervisory Control and Data Acquisition (SCADA) system every minute. Data are downloaded as Comma-Separated Values (CSV) files for further analysis. Because the thermal measurement instrument is installed outdoors, wireless communication (Wi-Fi) is employed to communicate between the instrument and the cloud-SCADA device.

The leaf temperature measurement instrument is shown in Fig. 1. The left picture shows the hardware unit consisting of AMG8833 as the thermal sensor unit, Raspberry Pi Zero W as the processing unit, an air temperature sensor, and a wireless communication unit. Meanwhile, the right picture shows the arrangement of leaf temperature measurements where the Dieffenbachia planted in a pot is the object of leaf measurement.

The AMG8833 is a low-cost thermal camera module with 64 infrared sensor arrays [23]. The array comprises eight columns and eight rows. This sensor measures the temperature of an object by measuring its thermal emission in the infrared spectrum. The points or pixels in the sensor array represent the temperatures of the detected object. The AMG8833 can measure the temperature between 0 and 80 °C with an accuracy of ± 2.5 °C. The module has a viewing angle of 600. It supports an Inter-Integrated Circuit (I2C) communication protocol for interfacing microcontroller systems. The price of AMG8833 is approximately US$41.

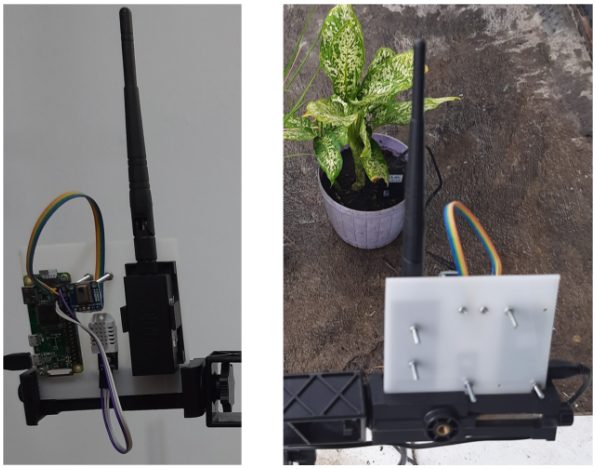

Fig. 1. Leaf temperature measurement instrument.

Raspberry Pi Zero W is a single-board computer suitable for embedded applications [24]. It has a 1 GHz single-core ARMv6 CPU (BCM2835) and 512MB of RAM. The price of the Raspberry Pi Zero W is approximately US$ 25. This small and affordable computer system is used to perform a real-time implementation of image segmentation techniques to measure leaf temperature.

In addition to the thermal camera, the DHT22 module and air temperature and humidity sensors are employed to measure the ambient temperature and humidity. The DHT22 has an operating range temperature of -40 to 80 °C with an accuracy of ± 0.5 °C. Air temperature provides valuable information for analyzing leaf temperatures.

B. Leaf Temperature Measurement Method

In a preliminary experiment, the collected thermal images show that the temperature of the leaf pixels is lower than that of the background. Based on this assumption, the researchers propose a method for measuring leaf temperature. A flowchart of the proposed leaf-temperature measurement method is shown in Fig. 2. It reads an 8×8 pixel thermal image from an AMG8833 thermal camera. It is noteworthy that the pixel value represents the temperature of the captured object. The next step is image segmentation, wherein an image is segmented into two groups: foreground and background. As described previously, the researchers consider the foreground to be a leaf object. Therefore, the leaf temperature can be calculated from the foreground pixels. After segmentation, the mean pixel value for each group is calculated. Because the mean minimum temperature represents the leaf object, it is the leaf temperature.

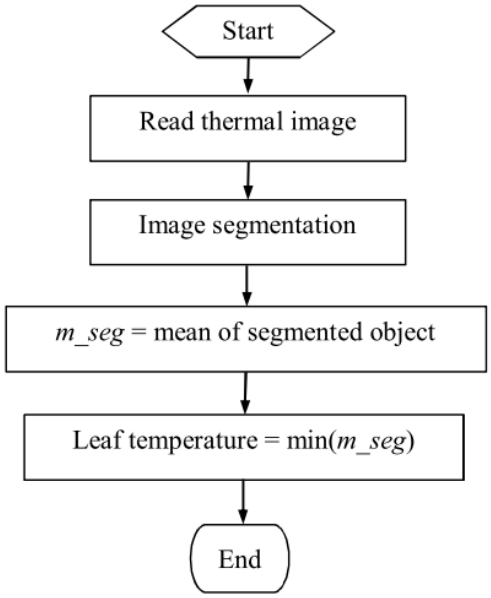

Fig. 2. Flowchart of proposed leaf temperature measurement.

The previous discussion clarifies that the accuracy of the proposed leaf temperature measurement method depends on the effectiveness of the segmentation techniques used to extract the foreground. Thus, in the research, the researchers evaluate two image-segmentation approaches: thresholding and clustering. The thresholding techniques used are Isodata, Li, Local, Mean, Minimum, Otsu, Triangle, and Yen. The clustering algorithms used are Ward Agglomerative, Average Agglomerative, Birch, Gaussian Mixture Model, K-Means, and Spectral.

In the thresholding technique, a threshold is used to separate the foreground and background in an image. In the research, the threshold is automatically defined using a specific algorithm as follows. Let the means of the foreground ($m_f(T)$) and background ($m_b(T)$) be defined in Eqs. (1) and (2), respectively. It has $pf(g)$ as the probability mass function, g as the image intensity ($g = 0, \ldots, 255$), and T as the threshold. Then, the Cumulative Distribution Function (CDF) is defined in Eq. (3).

$$m_f\,(T) = \sum_{g=0}^{T} g \times pf(g), \tag{1}$$

$$m_b\,(T) = \sum_{g=T+1}^{255} g \times pf(g), \tag{2}$$

$$cdf\,(g) = \sum_{i=0}^{g} pf(i). \tag{3}$$

The foreground ($\sigma_f^2(T)$) and background variances ($\sigma_b^2(T)$) are expressed in Eqs. (4) and (5), respectively. Based on Eqs. (1) to (5), the optimal threshold of the thresholding techniques is defined as follows. The optimal threshold (T_{opt}) of Isodata thresholding is defined in Eq. (6) [7].

$${\sigma_f}^2\,(T) = \sum_{g=0}^{T} [g - m_f(T)]^2 \times pf(g), \tag{4}$$

$${\sigma_b}^2\,(T) = \sum_{g=T+1}^{255} [g - m_b(T)]^2 \times pf(g), \tag{5}$$

$$T_{opt} = \lim_{n \to \infty} \frac{m_f(T_n) + m_b(T_n)}{2}. \tag{6}$$

Then, Li thresholding defines T_{opt} as expressed in Eqs. (7) and (8) [7]. In local thresholding, the optimal threshold at pixels (x, y) and $T_{opt}(x, y)$ is defined in Eq. (9) [7]. It shows $m_{wxw}(x, y)$ as the mean value over window size w of pixel (x, y) and C as a constant.

$$T_{opt} = argmin \left(\sum_{g=0}^{T} g \times pf(g) \times log \frac{g}{m_f(T)} + \sum_{g=T+1}^{255} g \times pf(g) \times log \frac{g}{m_b(T)} \right), \tag{7}$$

$$\sum_{g \leqslant T} g = \sum_{g \leq T} m_f(T)\ and\ \sum_{g \geq T} g = \sum_{g \geq T} m_b(T), \tag{8}$$

$$T_{opt}(x, y) = m_{w \times w}(x, y) - C. \tag{9}$$

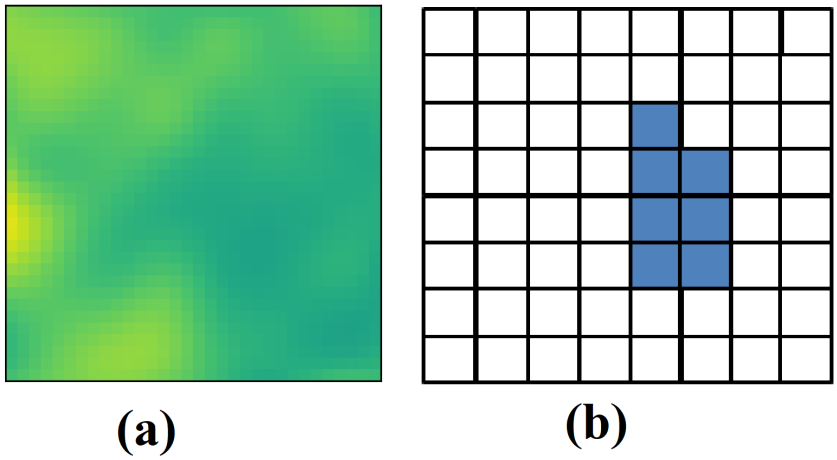

Fig. 3. Predefined leaf area for calculation of the leaf temperature: (a) Original thermal image and (b) Predefined leaf area in the 8×8 pixels of the thermal image.

Mean thresholding defines the optimal threshold T_{opt} as the integer part of Eq. (10) [7]. The y_g denotes the number of pixels with intensity g. Minimum thresholding defines an optimal threshold T_{opt} when Eq. (11) is satisfied [7]. The optimal threshold T_{opt} of Otsu thresholding is shown in Eq. (12) [7]. Triangle thresholding defines the optimal threshold T_{opt} based on the triangular property of the histogram. Then, Yen thresholding defines the optimal threshold T_{opt} as expressed in Eqs. (13)–(15) [7].

$$\frac{\sum_{g=0}^{255} g \times y_g}{\sum_{g=0}^{255} y_g}, \quad (10)$$

$$y_{T_{opt}} > y_{Topt-1} \; and \; y_{T_{opt}} \leqslant y_{T_{opt}+1}, \quad (11)$$

$$T_{opt} = argmax \{ \frac{cdf(T)\left(1-cdf(T)\right)\left(m_f(T)-m_b(T)\right)^2}{cdf(T)\sigma_f^2(T)+\left(1-cdf(T)\right)\sigma_b^2(T)} \}, \quad (12)$$

$$T_{opt} = argmax\{C_b(T) + C_f(T)\}, \quad (13)$$

$$C_b(T) = -log\{\sum_{g=0}^{T} \left(\frac{p(g)}{cdf(T)}\right)^2\}, \quad (14)$$

$$C_f(T) = -log\{\sum_{g=T+1}^{255} \left(\frac{p(g)}{1-cdf(T)}\right)^2\}. \quad (15)$$

Next, to measure the performance of the thresholding and clustering techniques, the researchers calculate the errors between the leaf temperature measurements, which are computed using the proposed method in Fig. 2, and the temperature measurements based on the predefined leaf area in the image. The predefined leaf area is manually determined by observing the thermal images, as illustrated in Fig. 3. Figure 3(a) shows the original thermal image, and the blue area in Fig. 3(b) is the predefined leaf area.

The measurement error ($meas\_err$) and absolute measurement error (abs_err) are expressed using Eqs. (16) and (17), respectively. It consists of $meas$ and $meas\_def$ as the leaf temperature measurements obtained using the proposed algorithm and the leaf temperature measurements based on the predefined leaf area, respectively.

$$meas\_err = \frac{meas - meas\_def}{meas\_def}, \quad (16)$$

$$abs\_err = \frac{|meas - meas\_def|}{meas\_def}. \quad (17)$$

III. Results and Discussion

The proposed leaf-temperature measurement techniques are evaluated using the collected thermal image dataset described in the previous section. The dataset contains 4,668 thermal images captured every minute during the day and night for five days. The proposed algorithm is implemented using Python and Scikit-Learn library [25].

Figure 4 shows examples of the segmentation results for a thermal image. Figure 4(a) shows a thermal image captured at 21:35. The segmented images using the Agglomerative Ward clustering, K-means clustering, and Otsu thresholding are shown in Figs. 4(b)–(d), respectively. The white pixels in Figs. 4(b)–(d) represent the lower-temperature class (or foreground), whereas the black pixels represent the higher-temperature class (or background). They show that the segmented images of the Agglomerative Ward (Fig. 4(b)) and K-Means clustering (Fig. 4(c)) are the same. However, they differ from the segmented image of Otsu thresholding (Fig. 4(d)).

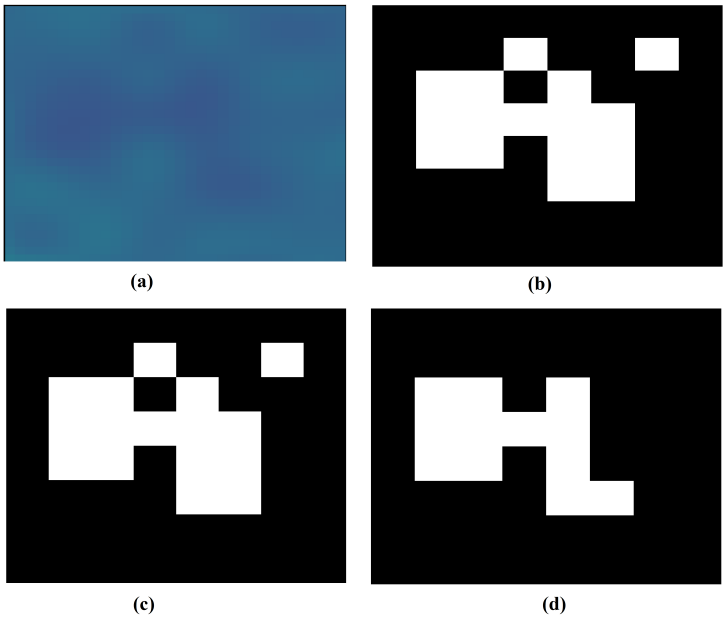

Fig. 4. Example of segmentation results: (a) Thermal image, (b) Agglomerative Ward clustering, (c) K-means clustering, and (d) Otsu thresholding.

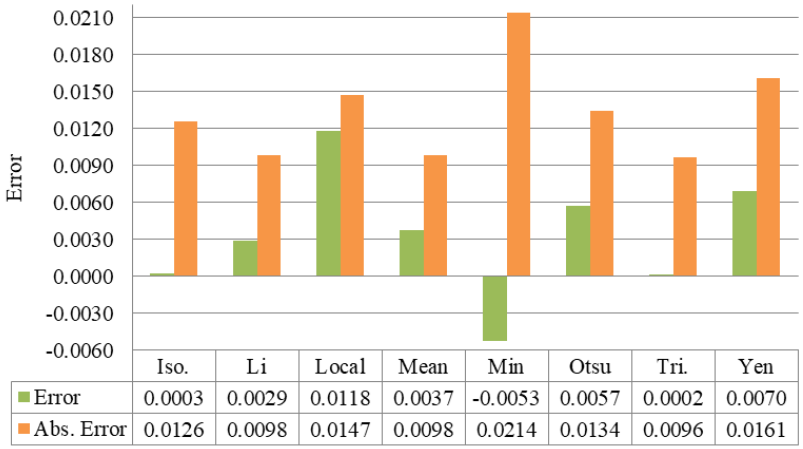

	Iso.	Li	Local	Mean	Min	Otsu	Tri.	Yen
Error	0.0003	0.0029	0.0118	0.0037	-0.0053	0.0057	0.0002	0.0070
Abs. Error	0.0126	0.0098	0.0147	0.0098	0.0214	0.0134	0.0096	0.0161

Fig. 5. Measurement errors of thresholding techniques in the daytime.

According to the algorithm described previously, the leaf temperature is calculated by averaging the temperature values of the white pixels. Since the Figs. 4(b) and (c) are the same, the leaf temperatures of both images are also the same. From the calculation using the proposed method, the leaf temperature is 25.84 °C. Meanwhile, the leaf temperature obtained by the proposed method in Fig. 4(d) is 25.72 °C. This result shows that, although the segmented images obtained by the different segmentation techniques differ, the calculated leaf temperatures are almost the same. Thus, the proposed leaf temperature measurement method effectively measures the leaf temperature from thermal images.

A. Comparison Results of Thresholding Techniques

The measurement errors for leaf temperature using thresholding techniques during day and night are illustrated in Figs. 5–7. The error (olive bar) is the average of the measurement errors calculated using Eq. (16). Then, absolute error (abs_error) (orange bar) is the average of the absolute measurement errors calculated using Eq. (17). Figure 5 shows that triangle thresholding achieves the lowest error of 0.0002

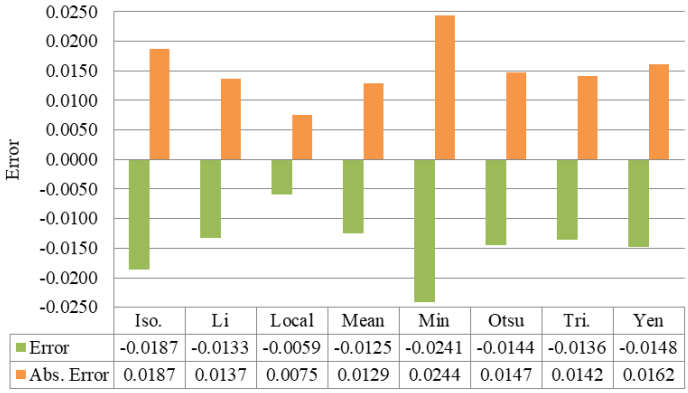

	Iso.	Li	Local	Mean	Min	Otsu	Tri.	Yen
Error	-0.0187	-0.0133	-0.0059	-0.0125	-0.0241	-0.0144	-0.0136	-0.0148
Abs. Error	0.0187	0.0137	0.0075	0.0129	0.0244	0.0147	0.0142	0.0162

Fig. 6. Measurement errors of thresholding techniques at nighttime.

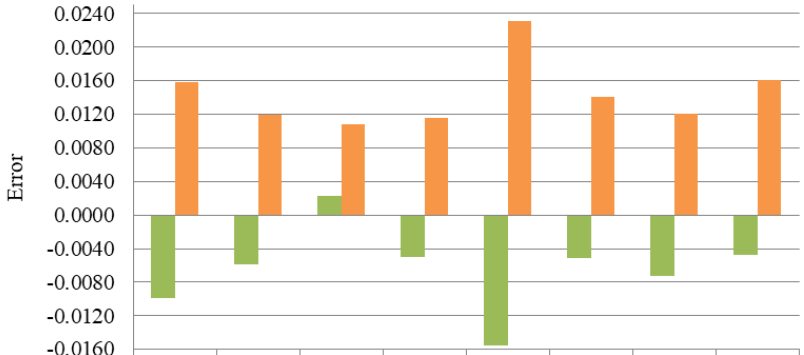

	Iso.	Li	Local	Mean	Min	Otsu	Tri.	Yen
Error	-0.0100	-0.0059	0.0023	-0.0050	-0.0155	-0.0052	-0.0073	-0.0048
Abs. Error	0.0159	0.0119	0.0109	0.0115	0.0231	0.0141	0.0121	0.0161

Fig. 7. Measurement errors of thresholding techniques in the day and nighttime.

and abs_error of 0.0096. Then, Fig. 6 shows that local thresholding has the lowest error of -0.0059 and abs_error of 0.0075. Additionally, Fig. 7 shows that local thresholding obtains the lowest error of 0.0023 and abs_error of 0.0109.

Figures 5 and 6 show that the leaf temperature measurement performance differs for day and night. Triangle thresholding achieves the best performance during the day, whereas local thresholding achieves the best performance during the night. Over the entire period, encompassing both day and night, as demonstrated in Fig. 7, local thresholding exhibits the most effective performance. Interestingly, the lowest abs_error in the day and night is higher than that in the day and night. This result means that no particular thresholding technique achieves the best performance during the day and night.

Figures 8 and 9 depict the temperature measurement profiles obtained using the thresholding techniques for five days and one day, respectively. They show that all thresholding techniques have similar behavior. In the sense compared to the reference, the values of measured leaf temperature are almost the same from 07:00 to 09:00, higher from 09:00 to 17:00, and lower from 17:00 to 07:00. The results show that in the morning (07:00–09:00), the temperatures of the extracted leaf objects are similar. Thus, the measured leaf temperatures are similar to those in reference. During the daytime (09:00–17:00), the temperatures of the objects in the background tend to be high. Therefore, when parts of the background are extracted as leaf objects, the measured leaf temperatures are higher than those of the reference. In contrast, the temperatures of the objects in the background are low during the night and early morning (17:00–07:00). Therefore, when parts of the background are extracted as leaf objects, the measured leaf temperatures are lower than those of the reference.

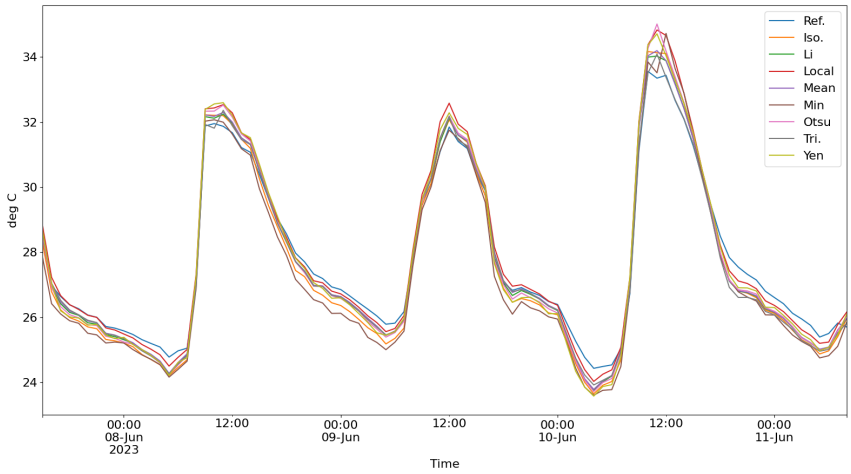

Fig. 8. Temperature measurement profiles using thresholding techniques during five days.

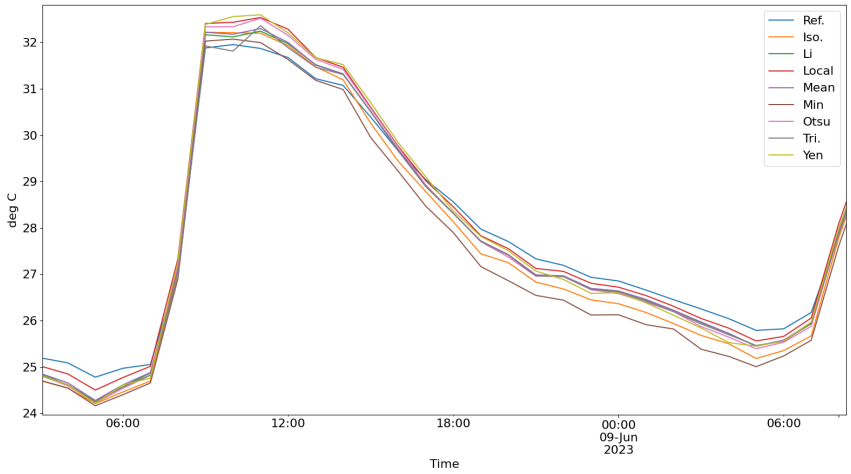

Fig. 9. Temperature measurement profiles using thresholding techniques during the day.

B. Comparison Results of Clustering Techniques

The errors in leaf temperature measurements using clustering techniques for day and night periods are presented in Figs. 10–12. The error (blue bar) is the average of the measurement errors calculated using Eq. (16). Meanwhile, abs_error (red bar) is the average of the absolute measurement errors calculated using Eq. (17).

Figure 10 shows that Agglomerative Ward clustering achieves the lowest error of 0.0061. Then, the lowest abs_error of 0.0135 is achieved by Agglomerative Ward And K-Means clustering. Figure 11 shows that the Birch clustering achieves the lowest error and abs_error of -0.0102 and 0.0125, respectively. Then, Fig. 12 shows that Birch clustering has the lowest error of 0.0004, and K-Means achieves the lowest abs_error of 0.0134.

Similar to the thresholding techniques, these results show that leaf temperature measurement performances are different during the day and night. Moreover, no particular thresholding technique achieves the best performance in day and night. Throughout the entire period, covering both day and night and considering the minimal errors, K-Means clustering demonstrates the best performance.

Figures 13 and 14 depict the temperature measurement profiles obtained using the clustering techniques for five days and a single day, respectively. The profiles exhibit behavior similar to that of the thresholding techniques discussed previously. For example, compared to the reference, the values of measured leaf temperature are almost the same from 07:00 to 09:00, higher from 09:00 to 17:00, and lower from 17:00 to 07:00.

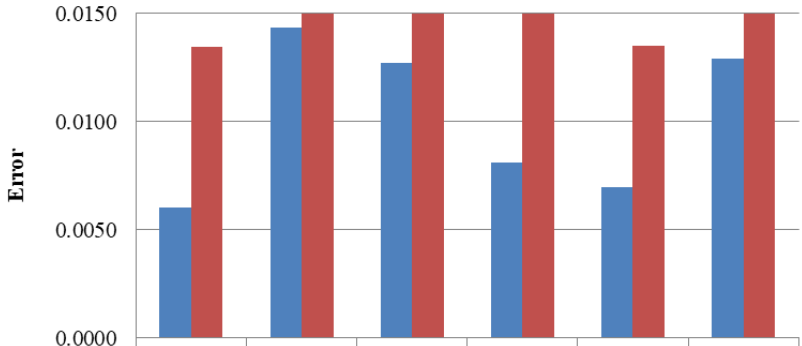

	Agg. Ward	Agg. Avg	Birch	Gauss. Mix.	K-Means	Spectral
Error	0.0061	0.0144	0.0127	0.0081	0.0070	0.0129
Abs. Error	0.0135	0.0252	0.0196	0.0159	0.0135	0.0200

Fig. 10. Measurement errors of clustering techniques in the daytime.

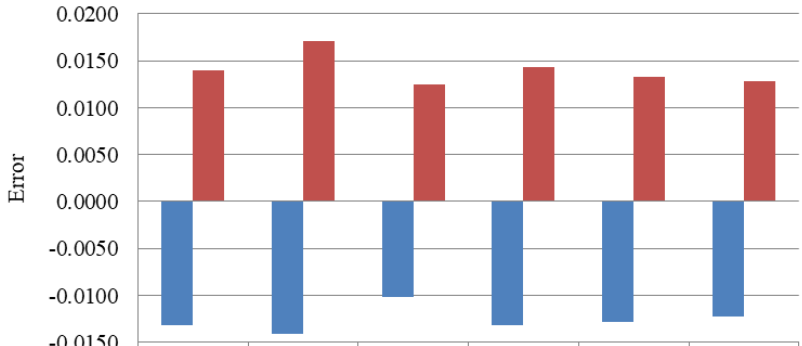

	Agg. - Ward	Agg.- Avg	Birch	Gauss. Mix.	K-Means	Spectral
Error	-0.0132	-0.0141	-0.0102	-0.0131	-0.0128	-0.0123
Abs. Error	0.0140	0.0170	0.0125	0.0143	0.0133	0.0128

Fig. 11. Measurement errors of clustering techniques at nighttime.

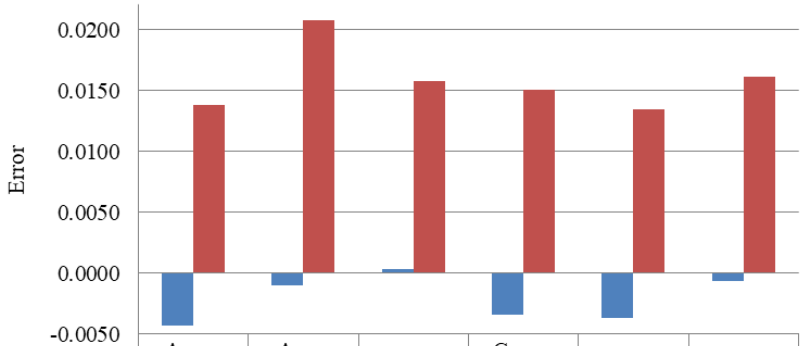

	Agg. - Ward	Agg.- Avg	Birch	Gauss. Mix.	K-Means	Spectral
Error	-0.0043	-0.0010	0.0004	-0.0034	-0.0037	-0.0007
Abs. Error	0.0138	0.0208	0.0158	0.0150	0.0134	0.0161

Fig. 12. Measurement errors of clustering techniques in the day and nighttime.

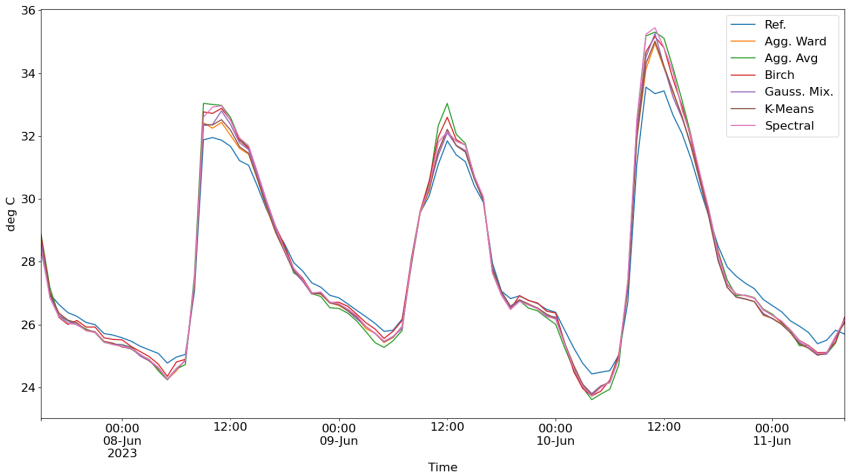

Fig. 13. Temperature measurement profiles using clustering techniques during five days.

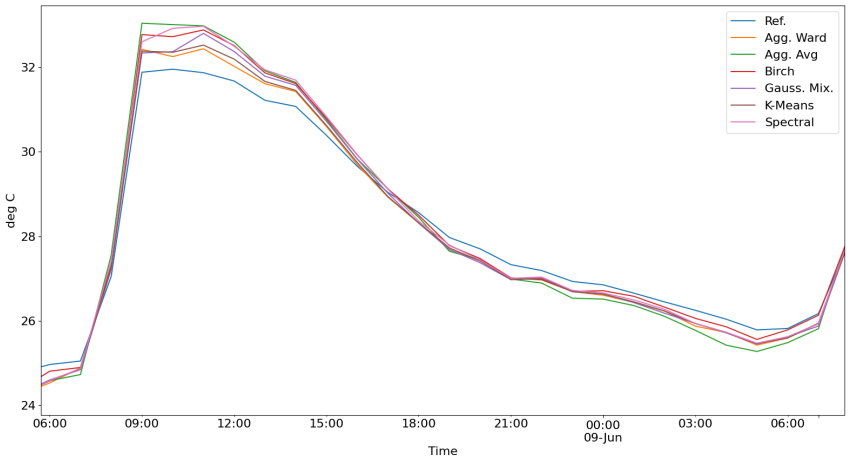

Fig. 14. Temperature measurement profiles using clustering techniques during the day.

TABLE II
COMPARISON TO EXISTING SYSTEMS.

References	Thermal Camera (Resolution)	Leaf Temperature Measurement	
		Method	Effectiveness
[14]	FLIR Vue Pro R (640×512 pixels)	Combined with RGB camera for leaf area detection	High cost, complex measurement
[15]	FLIR Lepton 3.5 (160×120 pixels)	Combined with RGB camera for leaf area detection	High cost, complex measurement
[17]	MLX90620 (16×4 pixels)	Leaf area measurement defined by the user manually	Low cost, manual measurement
Proposed Model	AMG8833 (8×8 pixels)	Leaf area detected by the thermal camera automatically	Low cost, automatic measurement

C. Comparison to Existing Systems

Table II shows a comparison of the existing systems. It shows that the proposed system is superior in two respects. First, it uses a low-cost and low-resolution thermal camera. Second, it provides efficient leaf temperature measurements using a single thermal camera for leaf area detection and temperature calculation.

IV. CONCLUSION

In conclusion, leaf temperature can be used to assess the health of a plant. Measuring or monitoring leaf temperatures is an effective method in precision

agriculture. Automatic leaf measurement systems using thermal cameras have recently become a challenging and interesting research topic.

In the research, a method for measuring leaf temperature using a thermal camera is developed. A low-resolution thermal camera is used to capture images of the leaves. Because the pixel values of the captured thermal image represent the temperature of the objects, the leaf temperature can be calculated by extracting the leaf area from the thermal image. Several image segmentation methods based on thresholding and clustering techniques have been used to extract leaf areas. The results show that most techniques achieve a low measurement error. However, local thresholding achieves the lowest error for the thresholding techniques, and k-means clustering has the lowest error for the clustering techniques.

In the future, the research can be extended to address more complex plants and environments. The algorithm and measurement instruments can also be improved accordingly. Furthermore, a real-time leaf temperature monitoring system can be implemented. Leaf temperature monitoring is an important part of the leaf monitoring system that can be used to monitor the plant's growth.

Acknowledgement

The research was supported by a Research Grant from the Ministry of Education, Culture, Research, and Technology, Republic of Indonesia in 2023 (No.: 077/E5/PG.02.00.PL/2023).

Author Contribution

Writing—original draft, A. S.; Methodology, A. S., and E. H.; Formal analysis, A. S.; Analysis result review, A. S., and E. H. All authors have read and agreed to the published version of the manuscript.

References

[1] C. J. Still, B. Rastogi, G. F. M. Page, D. M. Griffith, A. Sibley, M. Schulze, L. Hawkins, S. Pau, M. Detto, and B. R. Helliker, "Imaging canopy temperature: Shedding (thermal) light on ecosystem processes," *New Phytologist*, vol. 230, no. 5, pp. 1746–1753, 2021.

[2] W. Konrad, G. Katul, and A. Roth-Nebelsick, "Leaf temperature and its dependence on atmospheric CO2 and leaf size," *Geological Journal*, vol. 56, no. 2, pp. 866–885, 2021.

[3] T. M. Sexton, C. M. Steber, and A. B. Cousins, "Leaf temperature impacts canopy water use efficiency independent of changes in leaf level water use efficiency," *Journal of Plant Physiology*, vol. 258, p. 153357, 2021.

[4] M. Gräf, M. Immitzer, P. Hietz, and R. Stangl, "Water-stressed plants do not cool: Leaf surface temperature of living wall plants under drought stress," *Sustainability*, vol. 13, no. 7, pp. 1–11, 2021.

[5] D. H. Greer, "Leaf temperature and CO2 effects on photosynthetic CO2 assimilation and chlorophyll a fluorescence light responses during mid-ripening of Vitis Vinifera CV. Shiraz grapevines grown in outdoor conditions," *Functional Plant Biology*, vol. 49, no. 7, pp. 659–671, 2022.

[6] A. Soetedjo and E. Hendriarianti, "Leaf temperature monitoring system using low-cost thermal camera and IoT technology," in *2023 Second International Conference on Smart Technologies for Smart Nation (SmartTechCon)*. Singapore: IEEE, Aug. 18–19, 2023, pp. 183–188.

[7] ——, "A comparative study of Vetiveria Zizanioides leaf segmentation techniques using visible, infrared, and thermal camera sensors in an outdoor environment," *Applied System Innovation*, vol. 6, no. 1, pp. 1–27, 2022.

[8] G. Parihar, S. Saha, and L. I. Giri, "Application of infrared thermography for irrigation scheduling of horticulture plants," *Smart Agricultural Technology*, vol. 1, pp. 1–16, 2021.

[9] I. C. Hashim, A. . R. M. Shariff, S. K. Bejo, F. M. Muharam, K. Ahmad, and H. Hashim, "Application of thermal imaging for plant disease detection," in *IOP Conference Series: Earth and Environmental Science*, vol. 540, no. 1. IOP Publishing, 2020.

[10] K. H. Son, H. S. Sim, J. K. Lee, and J. Lee, "Precise sensing of leaf temperatures for smart farm applications," *Horticulturae*, vol. 9, no. 4, pp. 1–16, 2023.

[11] K. Iseki and O. Olaleye, "A new indicator of leaf stomatal conductance based on thermal imaging for field grown cowpea," *Plant Production Science*, vol. 23, no. 1, pp. 136–147, 2020.

[12] M. Pineda, M. Barón, and M. L. Pérez-Bueno, "Thermal imaging for plant stress detection and phenotyping," *Remote Sensing*, vol. 13, no. 1, pp. 1–21, 2020.

[13] C. Still, R. Powell, D. Aubrecht, Y. Kim, B. Helliker, D. Roberts, A. D. Richardson, and M. Goulden, "Thermal imaging in plant and ecosystem ecology: Applications and challenges," *Ecosphere*, vol. 10, no. 6, pp. 1–16, 2019.

[14] Z. Zhou, G. Diverres, C. Kang, S. Thapa, M. Karkee, Q. Zhang, and M. Keller, "Ground-based

thermal imaging for assessing crop water status in grapevines over a growing season," *Agronomy*, vol. 12, no. 2, pp. 1–12, 2022.

[15] J. Giménez-Gallego, J. D. González-Teruel, F. Soto-Valles, M. Jiménez-Buendía, H. Navarro-Hellín, and R. Torres-Sánchez, "Intelligent thermal image-based sensor for affordable measurement of crop canopy temperature," *Computers and Electronics in Agriculture*, vol. 188, pp. 1–11, 2021.

[16] B. Kim, "Design and implementation of low-cost thermal-RGB camera for remote monitoring crop," *Global Journal of Engineering Sciences*, vol. 8, no. 5, pp. 8–10, 2021.

[17] M. Noguera, B. Millán, J. J. Pérez-Paredes, J. M. Ponce, A. Aquino, and J. M. Andújar, "A new low-cost device based on thermal infrared sensors for olive tree canopy temperature measurement and water status monitoring," *Remote Sensing*, vol. 12, no. 4, pp. 1–20, 2020.

[18] P. N. Tan, M. Steinbach, A. Karpatne, and V. Kumar, *Introduction to data mining (Second edition)*. Pearson, 2019.

[19] E. Kokin, M. Pennar, V. Palge, and K. Jürjenson, "Strawberry leaf surface temperature dynamics measured by thermal camera in night frost conditions," *Agronomy Research*, vol. 16, no. 1, pp. 122–133, 2018.

[20] M. Mejia-Herrera, J. S. Botero-Valencia, D. Betancur-Vásquez, and E. A. Moncada-Acevedo, "Low-cost system for analysis pedestrian flow from an aerial view using near-infrared, microwave, and temperature sensors," *HardwareX*, vol. 13, pp. 1–14, 2023.

[21] C. Perra, A. Kumar, M. Losito, P. Pirino, M. Moradpour, and G. Gatto, "Monitoring indoor people presence in buildings using low-cost infrared sensor array in doorways," *Sensors*, vol. 21, no. 12, pp. 1–19, 2021.

[22] S. Lu and E. Cochran Hameen, "An interactive task conditioning system featuring personal comfort models and non-intrusive sensing techniques: A field study in Shanghai," *Technologies*, vol. 9, no. 4, pp. 1–17, 2021.

[23] Panasonic Industry, "Grid-EYE® infrared array sensor." [Online]. Available: https://na.industrial.panasonic.com/products/sensors/sensors-automotive-industrial-applications/lineup/grid-eye-infrared-array-sensor

[24] Raspberry Pi, "Raspberry Pi Zero W." [Online]. Available: https://www.raspberrypi.com/products/raspberry-pi-zero-w/

[25] F. Pedregosa, G. Varoquaux, A. Gramfort, V. Michel, B. Thirion, O. Grisel, M. Blondel, P. Prettenhofer, R. Weiss, V. Dubourg, J. Vanderplas, A. Passos, D. Cournapean, M. Brucher, M. Perrot, and E. Duchesnay, "Scikit-learn: Machine learning in python," *The Journal of Machine Learning research*, vol. 12, pp. 2825–2830, 2011.